Infiltrating monocytes trigger EAE progression but fail to contribute to the resident microglia pool

Ajami B, Bennett JL, Krieger C, McNagny KM, Rossi FMV.

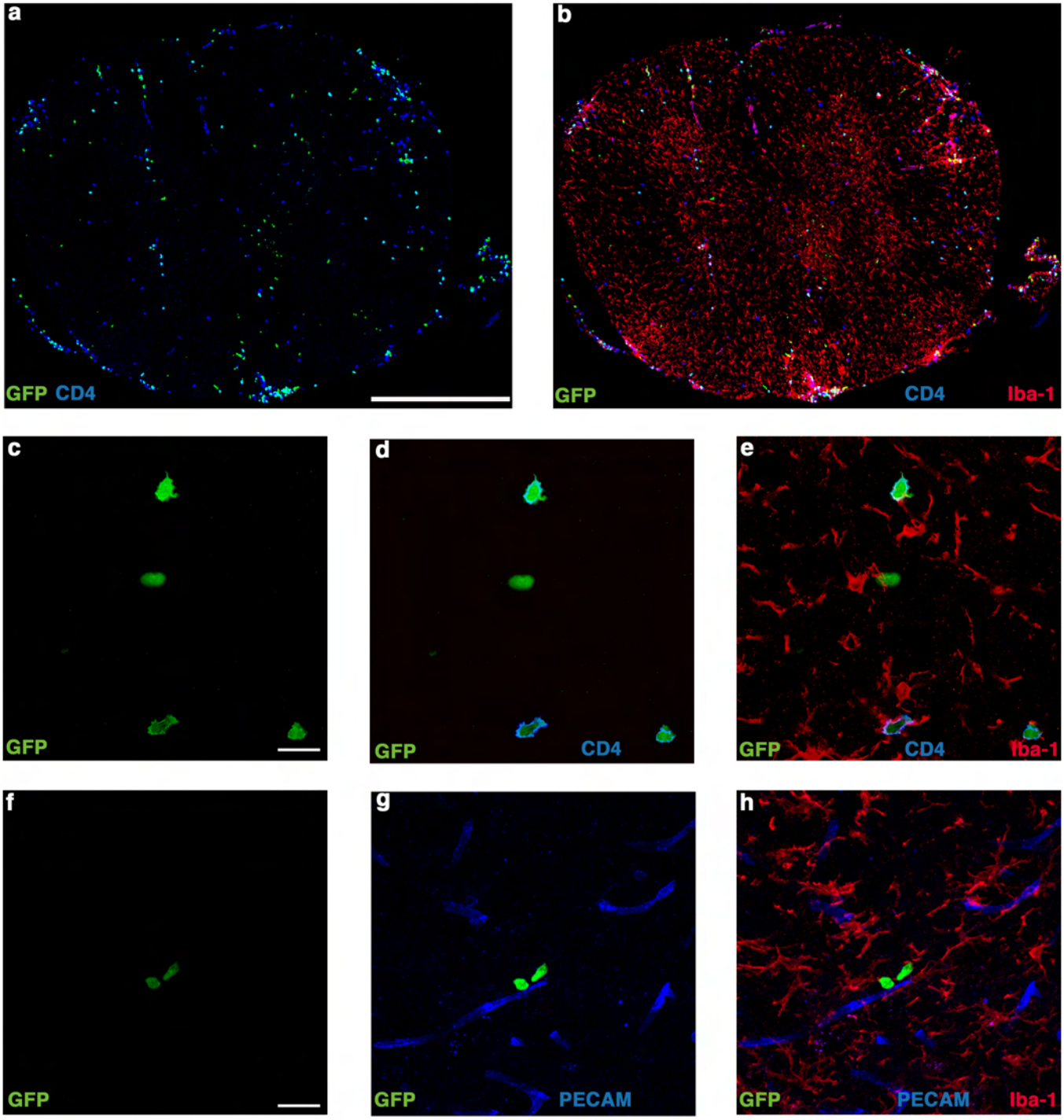

Supplementary figure 1: Efficient entry of partner-derived T–lymphocytes, but not myelomonocytic cell in the spinal cords of EAE-induced parabionts.

(a–e) Distribution of GFP$^+$ partner-derived cells (green) CD4$^+$ lymphocytes (blue), and Iba-1$^+$ microglia in the spinal cord of a GFP$^-$ parabiotic mouse two weeks after immunization with myelin antigens.**(a,b)** Collage of maximum intensity projections of confocal image stacks showing a view of the entire spinal cord. The rare "yellow" appearing cells are due to the overlap of a green and a red cell present in different optical sections. Scale bars: 500μm.**(c–e)** Individual optical sections confirm that the majority of the GFP$^+$ cells (green) stain for CD4 (blue) and that none of the GFP$^+$ cells expressed Iba–1 (red). Scale bar: 50μm.**(f–h)** Spinal cord sections were stained for the microglial marker Iba–1 (red) and the endothelial marker PECAM (blue). Partner derived GFP$^+$ cells (green) were readily observed outside of the blood vessels in the spinal cords of parabiotic mice affected by EAE. However, none of the GFP$^+$ cells was also positive for Iba–1. Scale bars: 50μm.

Nature Neuroscience: doi:10.1038/nn.2887

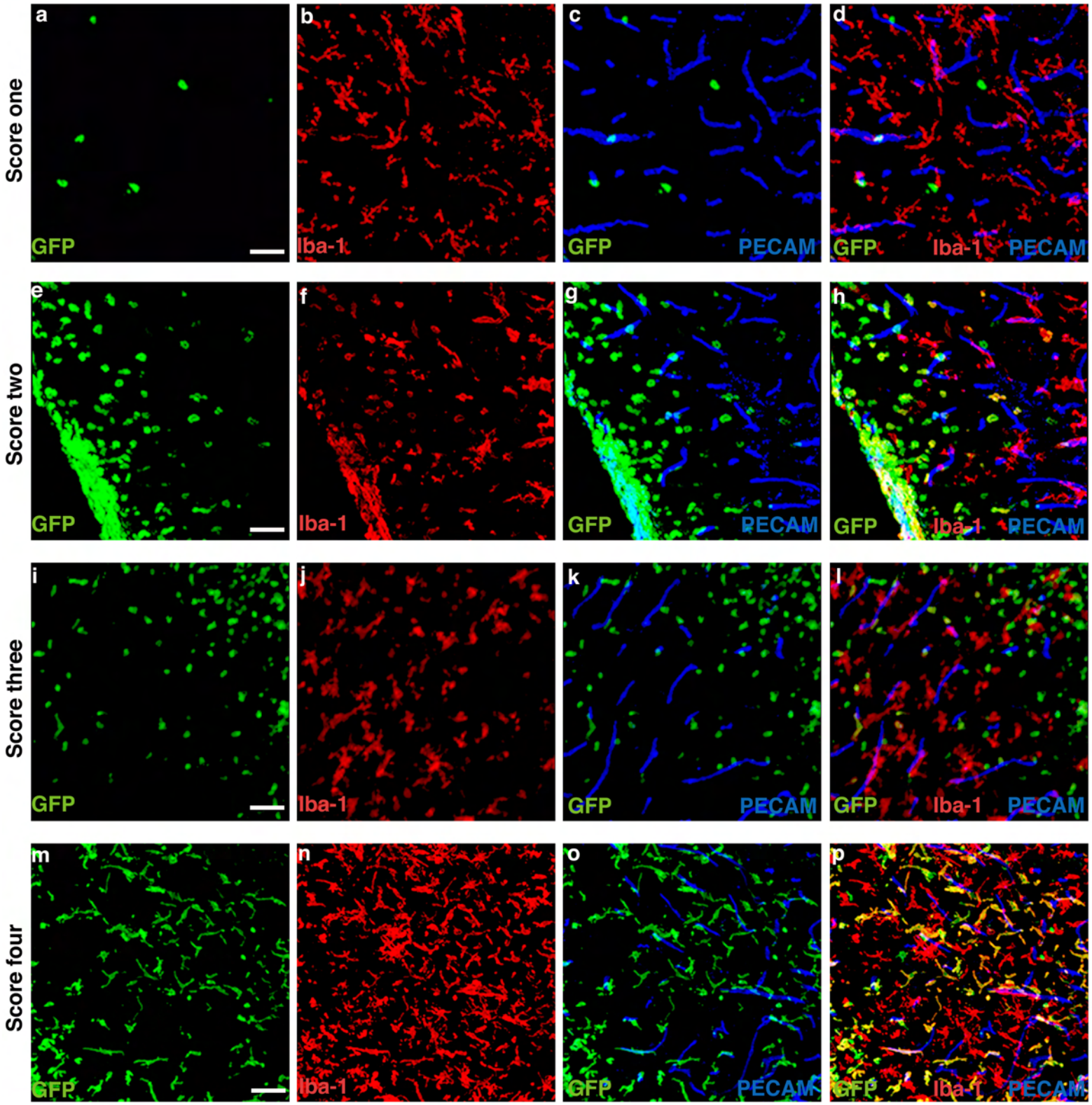

Supplementary figure 2: Blood–derived inflammatory cells are recruited to the diseased CNS and their increased number correlates with the disease progression.

(a–p) Higher magnifications of the boxed areas in figure two. The panels show increased cell number and changes in the morphology of GFP^+ cells as the disease progress to score four.

Iba–1:Red , GFP: green, PECAM: Blue. Scale bars: 50 μm

Nature Neuroscience: doi:10.1038/nn.2887

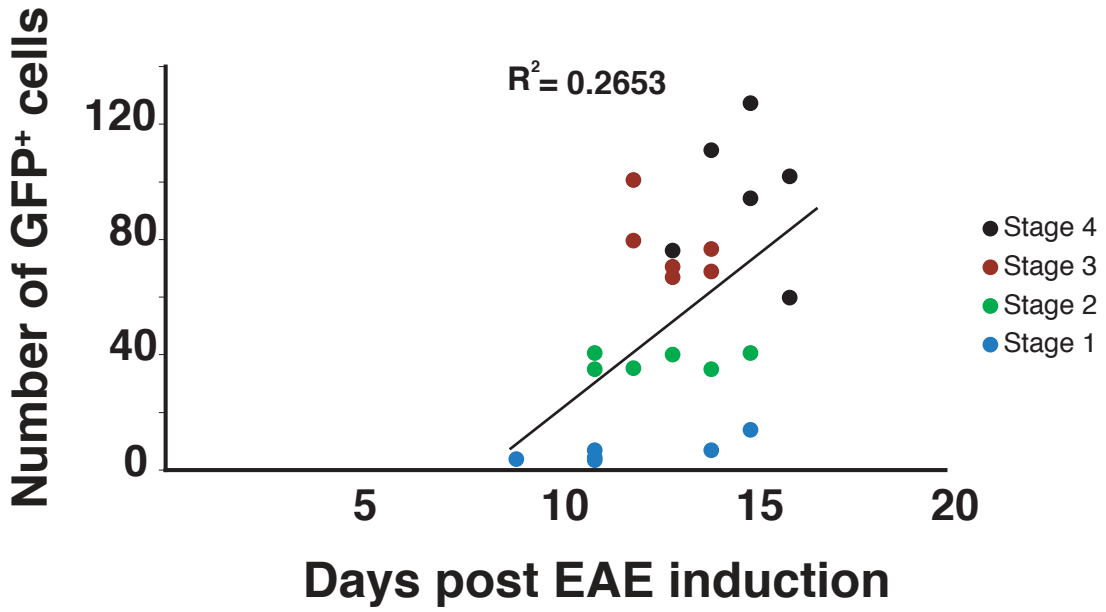

Supplementary figure 3: The number of blood–derived inflammatory cells found in spinal cord sections does not correlate with the time between EAE induction and tissue analysis.

Nature Neuroscience: doi:10.1038/nn.2887

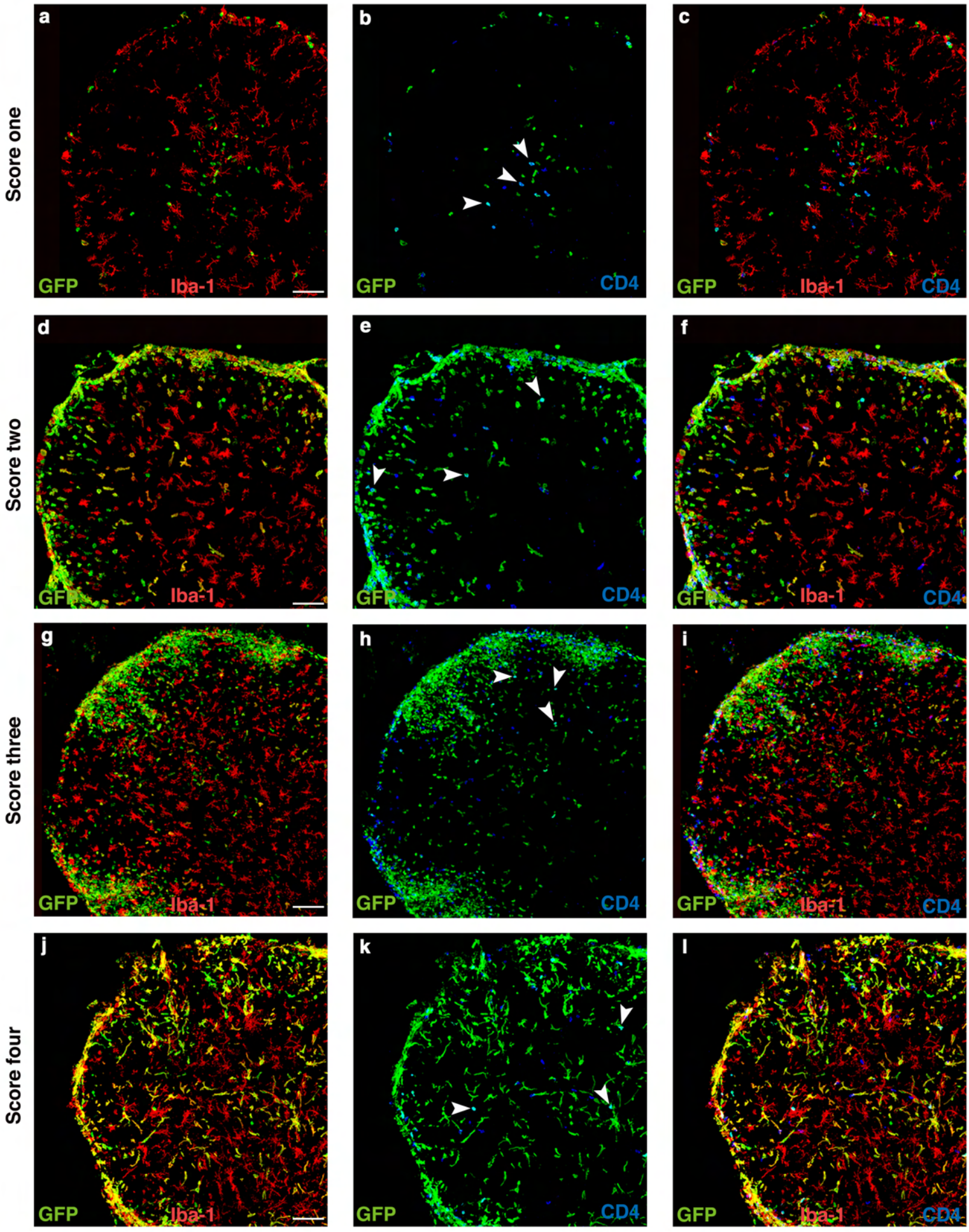

Nature Neuroscience: doi:10.1038/nn.2887

Supplementary figure 4: $CD4^+$ lymphocytes are found in the spinal cord at all stages of EAE. (a–l) Collages of confocal optical sections of the spinal cord of irradiated/separated parabionts at each clinical score of EAE. Macrophages/microglia are identified by staining for Iba–1 (red), CD4 staining is shown in blue and partner–derived cells are identified by GFP (green). Arrowheads indicate representative partner–derived lymphocytes. Scale bars: 100μm.

Nature Neuroscience: doi:10.1038/nn.2887

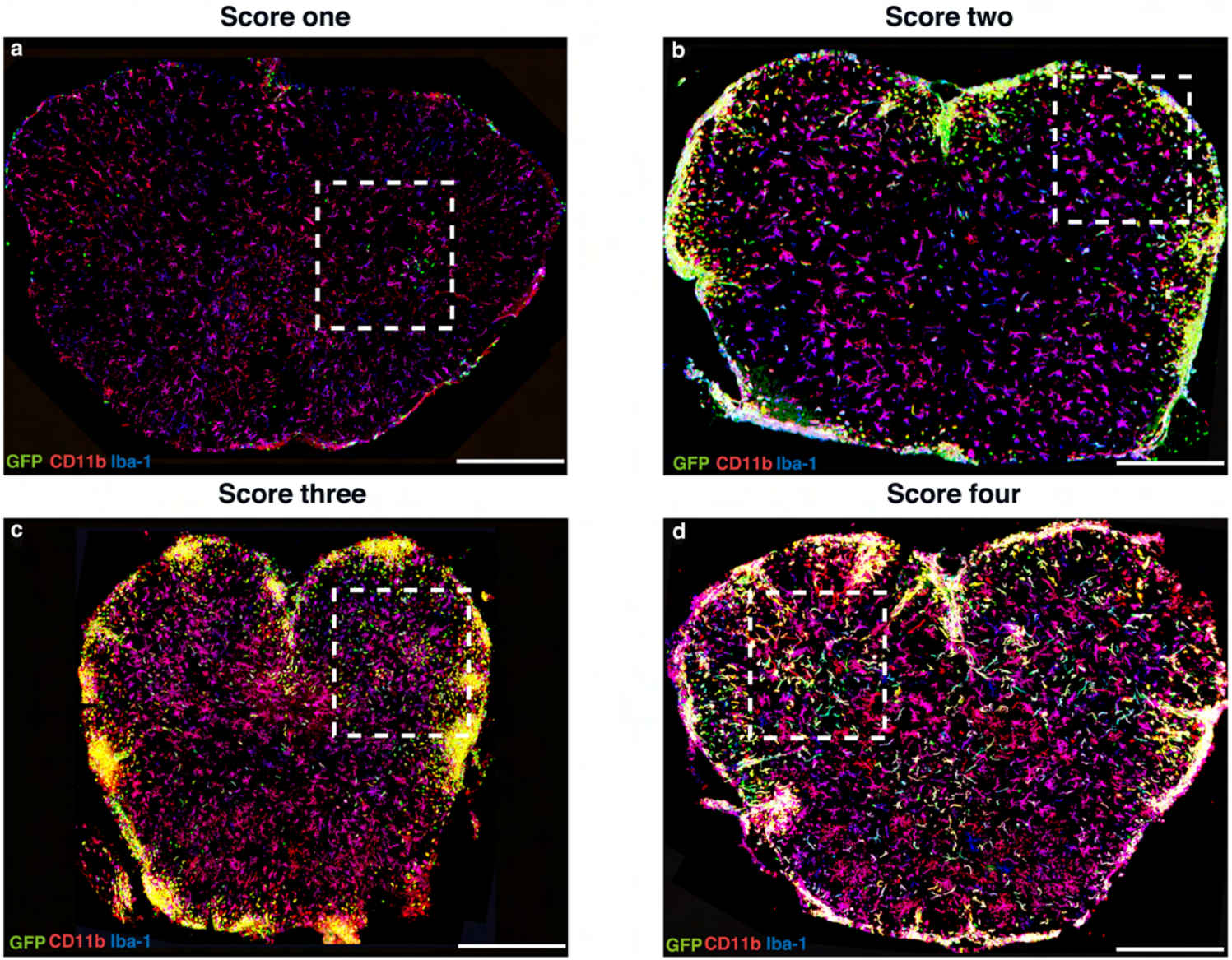

Supplementary figure 5: Phenotype of infiltrating myelomonocytic cells at different stages of disease progression.

(a–d) Collages of maximum intensity projections of confocal image stacks showing a view of the entire spinal cord of mice at different stages of EAE. Scale bars: 500 μm.

Higher magnification and split channel images of boxed areas at each time point are shown in figure three.

Iba–1: Blue, GFP: green, CD11b: Red

Nature Neuroscience: doi:10.1038/nn.2887

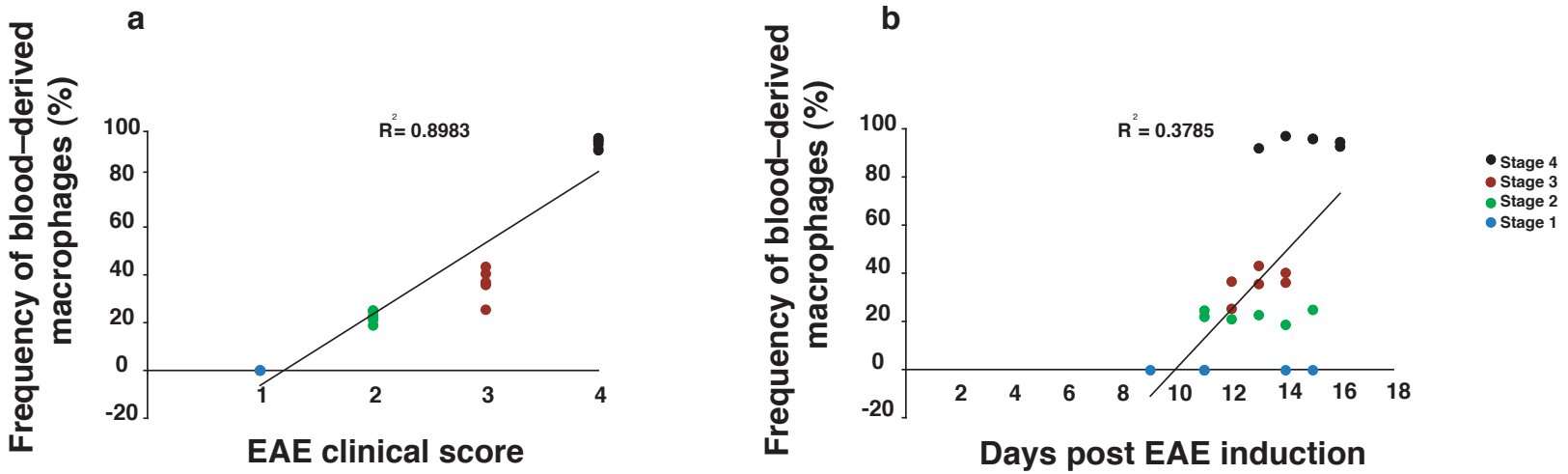

Supplementary Figure 6:Differentiation of infiltrating inflammatory monocytes to macrophages after entry into the CNS correlates with disease progression rather than time elapsed from EAE iduction.
(a) shows a strong correlation between the increase in numbers of blood derived macrophages and the severity of EAE (N=6). In contrast **(b)** shows that the appearance of blood derived macrophages does not correlate with time post EAE induction (N=6).

Nature Neuroscience: doi:10.1038/nn.2887

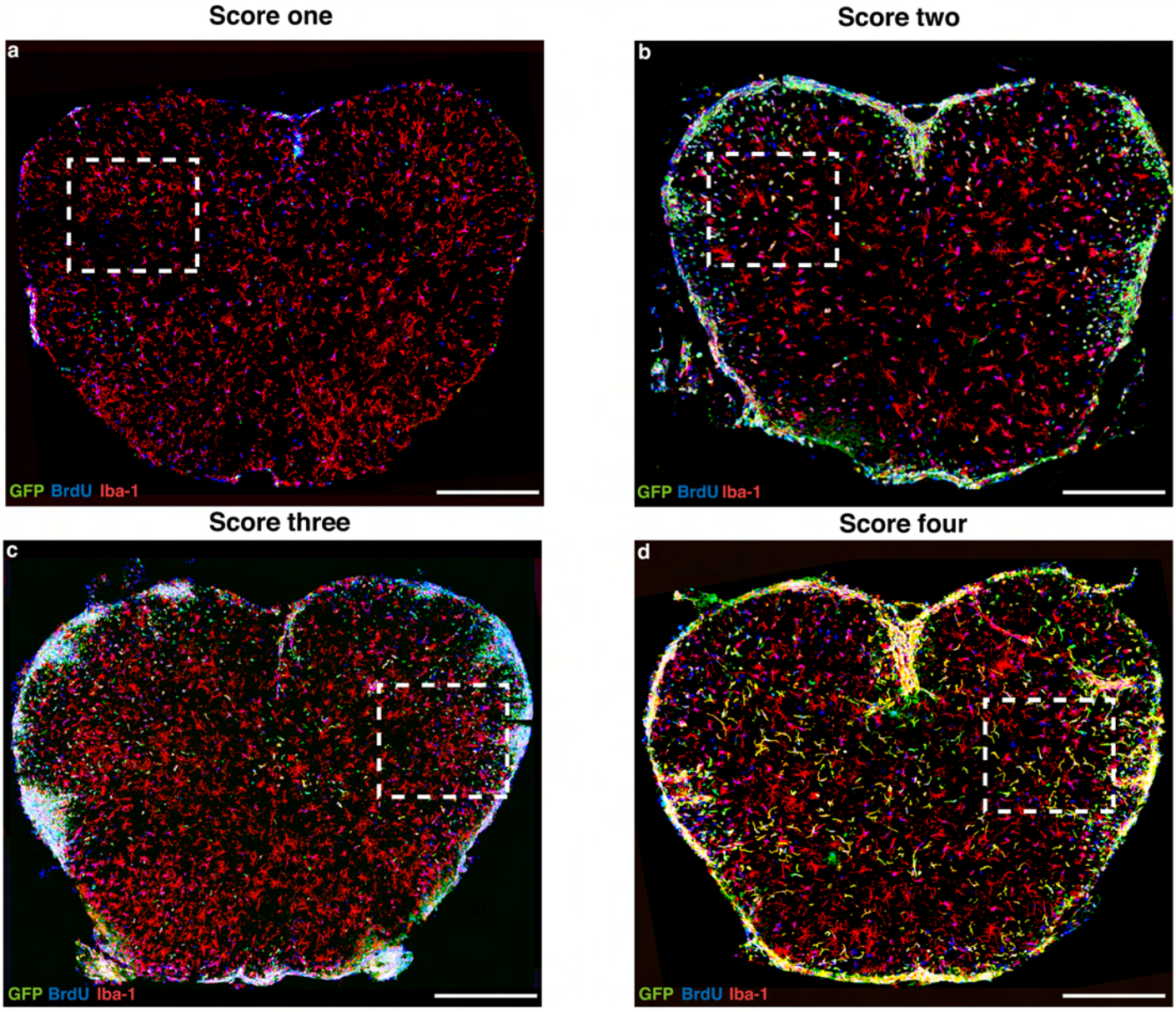

Supplementary figure 7: Proliferation of resident microglia during disease progression.
(a,b,c,d) Representative spinal cord sections of EAE–induced mice at four different clinical scores of the disease. Each panel shows a collage of maximum intensity projections of confocal image stacks showing a view of the entire spinal cord. A higher magnification and split channel images of boxed areas at each time point are shown in figure four. GFP: green, BrdU: blue, Iba–1: red. Scale bars: 500 μm.

Nature Neuroscience: doi:10.1038/nn.2887

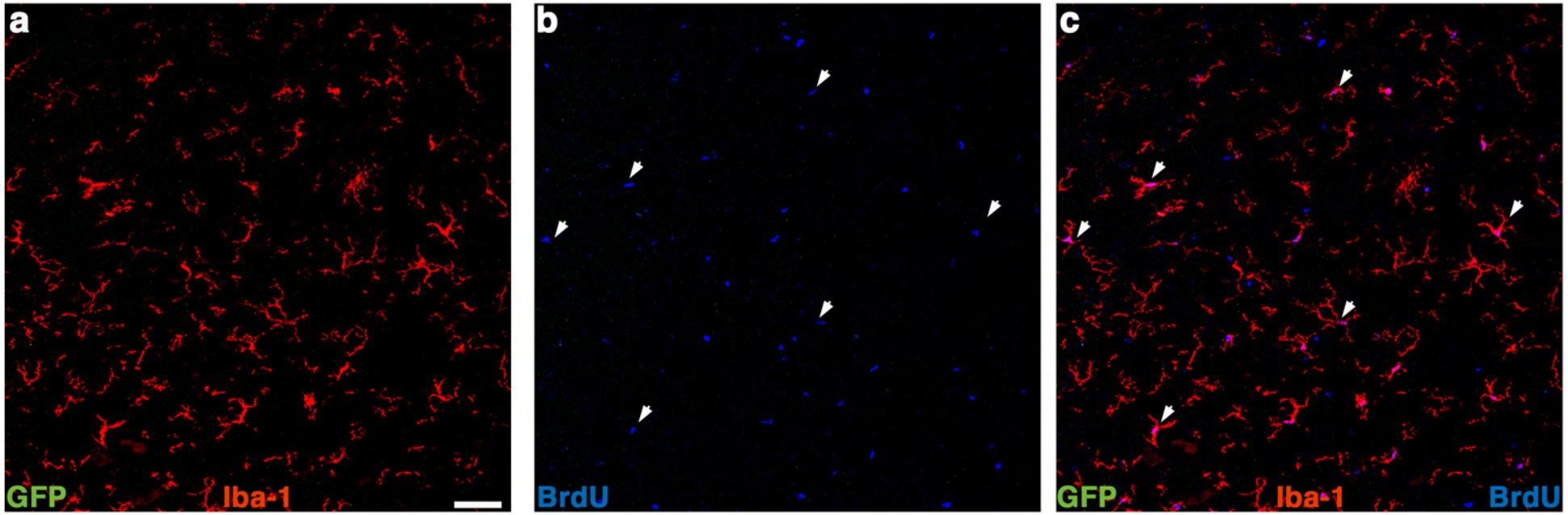

Supplementary figure 8: Endogenous microglia activation precedes the entry of blood–derived inflammatory cells in the CNS of EAE–induced mice.

(a,b,c) Confocal analysis shows the incorporation of BrdU in Iba–1^{+} cells in the absence of partner–derived GFP^{+} cells indicating that activation of resident microglia takes place prior to blood–derived inflammatory cell infiltration. Scale bars: 50 μm

Iba–1: Red. GFP: Green, BrdU: Blue

Nature Neuroscience: doi:10.1038/nn.2887

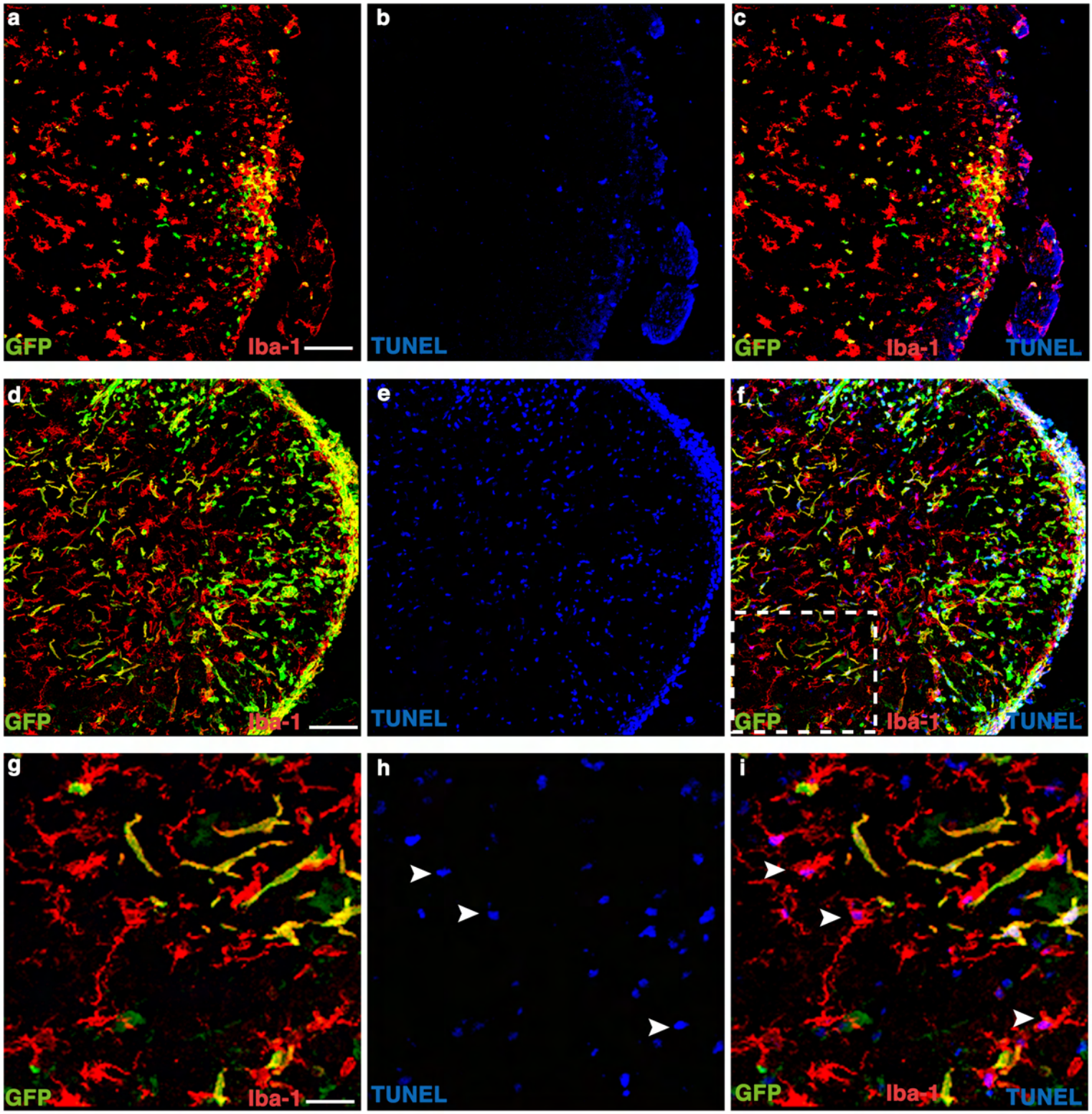

Supplementary Figure 9: Endogenous microglia undergo apoptosis between clinical scores 3 and 4 of EAE.

(a–i) TUNEL staining in spinal cord sections of chimeric mice at score three and four of EAE disease. TUNEL positive (blue) endogenous microglia ($Iba1^{+}$, GFP^{-}) is readily detectable at score four **(d–i)** but not at score three **(a–c)** disease suggesting apoptosis as the possible mechanism for the observed decline in microglia number between the two scores. **(g–i)** shows a higher magnification view of the boxed area in panel f.
TUNEL: blue, GFP: green, Iba–1: red. Scale bar **(a–f)**: 100 μm. Scale bar **(g–i)**: 50 μm.

Nature Neuroscience: doi:10.1038/nn.2887

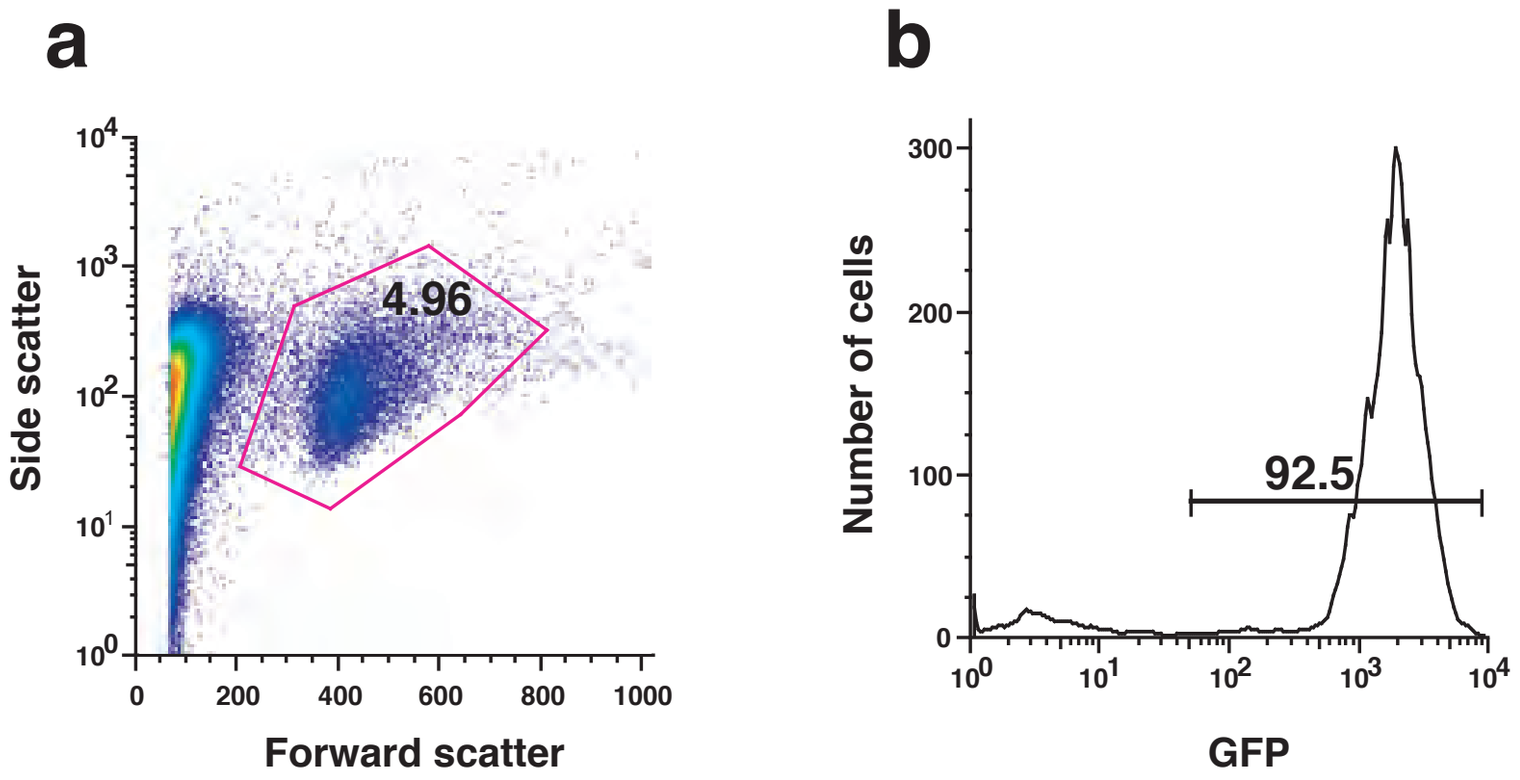

Supplementary Figure 10:Analysis of chimerism in peripheral blood by flow cytometry:

(a) Representative plot showing the gating of the main population of cells in peripheral blood. Low forward scatter events represent erythrocytes and platelets remaining after lysis and are excluded from further analysis. **(b)** Representative plot showing the gating used to calculate the percentage of GFP^+ cells within the main population shown in panel a.

Nature Neuroscience: doi:10.1038/nn.2887

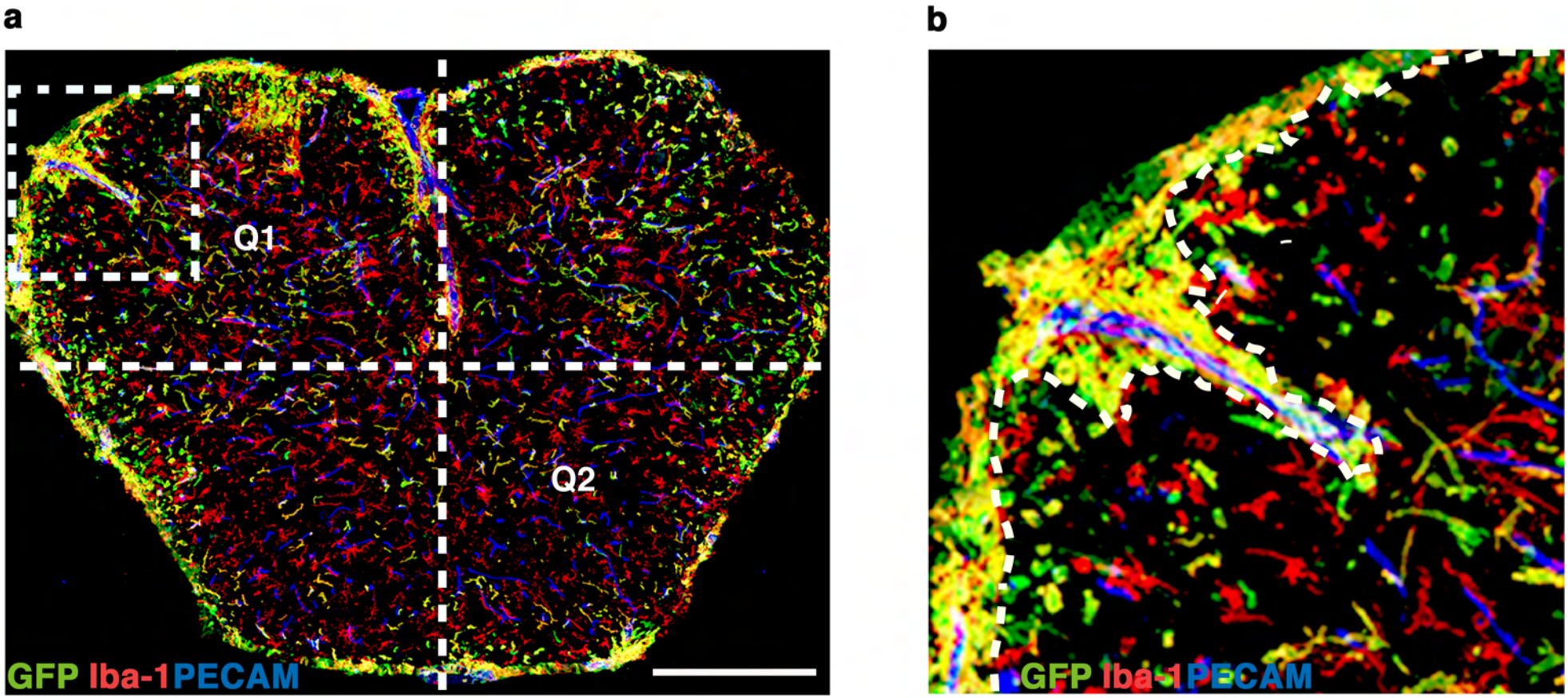

Supplementary figure 11: Schematic description of the counting method used to quantify stained cells in spinal cord sections.

(a) Two opposite quadrants (Q1 and Q2) were counted in each spinal cord section. **(b)** Higher magnification view of the boxed area indicated in panel **(a)**. The cells to the left of the dashed area were considered associated with the meninges rather than with the parenchyma, and were not included in the counts.

Nature Neuroscience: doi:10.1038/nn.2887

	EAE Clinical Score	One	Two	Three	Four
a	**Average total number of GFP^+ cells**	**5.4** ±3.5	**37.8** ±11.3	**77.2** ±22.4	**95.1** ±29.7
b	**Average total number of macrophages ($GFP^+/Iba\text{-}1^+$)**	**0**	**8.4**±2.9	**26.8**±6.8	**90.1**±29.7
c	**Mean Percentage of blood-derived macrophages (GFP^+ / $Iba\text{-}1^+$)**	**0**	**22.5**±5.2	**36.4**±10.6	**94.9**±3.3
d	**Mean percentage of blood-derived monocytes (GFP^+ / CD11b+/$Iba\text{-}1^-$)**	**0**	**59**±8.6	**71**±12.9	**17**±8.2

	EAE Clinical Score	One	Two	Three	Four
a	**Average total number of microglia ($Iba\text{-}1^+$)**	**60.4** ±18.2	**75.9** ±23.2	**154.4** ±29.21	**94** ±33.9
b	**Mean Percentage of $BrdU^+$ microglia ($BrdU^+/Iba\text{-}1^+$)**	**22.3**±6.2	**22.7**±5.5	**61.1**±13.6	**61.3**±13.4

Supplementary Table 1: Individual data points used to calculate averages presented in the main figures.

Infiltration of blood–derived inflammatory cells increased as the disease progress to the paralytic stages (Fig 2, 3, 4). Two opposite quadrants in each spinal cord section were counted. The data represent average mean ± s.d.

P values for each comparison point are as follow:

(a) Average absolute number of GFP^+ cells **(Fig 2a)**. P value between score one and two: 7.06E–20; between score two and three: 7.77E–13; between score three and four: 0.005.

(b) Percentage of blood derived monocytes **(Fig 3a)**. P value between score one and two: 5.74E–16; Score two and three: 0.003; score three and four: 4.62E–15.

(c) Percentage of blood derived macrophages **(Fig 3b)**. P value between score one and two: 1.81E–24; score two and three: 4.66E–09; score three and four: 7.49E–31.

(d) Average absolute number of macrophages **(Fig 4b)**. P value between score one and two: 8.17E–19; between score two and three: 2.24E–19; between score three and four: 2.52E–15.

Activation of microglia precedes the infiltration of blood derived inflammatory cells (Fig 4). Two opposite quadrants in each spinal cord section were counted. The data represent average mean ± s.d.

P value for each comparison point is as follow:

(a) Average absolute number of microglia **(Fig 4b)**. P value between score one and two: 0.002; between score two and three: 2.2E–19; between score three and four: 1.20E–11.

(b) Percentage of $BrdU^+$ microglia **(Fig 4a)**. P value between score one and two: 0.77; between score two and three: 4.41E–20; between score three and four: 0.94.